International Journal of New Horizons in Physics

http://dx.doi.org/10.12785/ijnhp/010102

Crystallization rate and Avrami index of different composition of $Se_{80-x}Te_{20}Sb_x$

***E. R. Shaaban*[1,*], *H. A. Elshaikh*[2] *and M. M. Soraya*[2]**

[1]Department of Physics, Faculty of Science, Al-Azhar University, Assuit, Egypt.
[2]Department of Physics, Faculty of Science, Aswan University, Aswan, Egypt.

Received: 10 Feb 2014 , Revised: 27 March 2014, Accepted: 2 April 2014
Published online: 1 July 2014

Abstract: Crystallization kinetics of $Se_{80-x}Te_{20}Sb_x$ (x= 0, 2, 4, 6, 8, 10) glassy compositions have been investigated using differential scanning calorimetry under non-isothermal conditions. The kinetic parameters as activation energy of glass transition and activation energy of crystallization have been determined. It was found a gradual increase of these parameters with increasing the *Sb* content within the composition, this trend was attributed to the larger atomic weight of *Sb* in comparison with that of *Se*. The nucleation and growth morphology have been determined through the theoretical work that introduced by Johnson, *Mehl* and *Avrami (JMA model)*. According to the average values of *Avrami* indices, $< n >$, $Se_{20}Te_{80}$ has volume nucleation, one dimensional growth and the other remaining compositions have volume nucleation, two dimensional growth. These results of *Avrami* indices were emphasized through an investigation of crystalline phases a cross thermal treatment using X-rays diffraction.

Keywords: Crystallization rate, Avrami index

1 Introduction

Chalcogenide glasses are a popular family of inorganic glassy materials which always contain one or more of the chalcogen elements: *S*, *Se* or *Te* in conjunction with more electropositive elements like As and Ge, but also *P*, *Sb*, *Bi*, *Si*, *Sn*, *Pb*, *B*, *AI*, *Ga*, *In*, *Tl*, *Ag*, lanthanides and *Na*. A lot of works have been done to study the structure, electrical properties, photoconductivity, glass formation and crystallization kinetics of the chalcogenide glasses [1, 2, 3, 4, 5, 6, 7, 8].

The current interest in chalcogenide materials centers on X-ray imaging [9], xerography [10], optical recording [11], memory switching [12] and electrographic applications such as photoreceptors in photocopying and laser printing [13, 14, 15]. *Se-Te* glassy alloys have drawn great importance among chalcogenide glasses, because of their higher photosensitivity, greater hardness, higher crystallization temperature and smaller ageing effects as compared to pure Se glass for better applications [16]. Furthermore, the addition of third element to *Se-Te* alloys can improve their properties and make them more suitable for various applications. It was observed that the DC conductivity increases, the activation energy for DC conduction decreases, the thermoelectric power decreases and the photoconductive decay becomes slower on incorporation of *Sb* into binary *Se-Te* alloys [17, 18, 19, 20, 21, 22], which was attributed to that the addition of *Sb* to the *Se-Te* system leads to a cross-linking of the *Se-Te* chains increasing the disorder in the system and hence leads to a deeper penetration of the localized states into the energy gap. For a good information about the resistance switching behavior in these glasses, as the type of switching (threshold or memory), crystallization studies may be useful in this region, depending upon the rate of crystallization [23].

In the present work crystallization kinetics of $Se_{80-x}Te_{20}Sb_x (x = 0, 2, 4, 6, 8, 10)$ have been investigated under non-isothermal conditions, the nucleation and growth morphology have been determined through the *JMA* model. Also other kinetic parameters like activation energy of crystallization and activation energy for glass transition have been determined. Identification of the phases at which the alloy crystallize after thermal process has been proposed using X-rays diffraction.

* Corresponding author e-mail: esam_ramadan2008@yahoo.com

2 Experimental details

Se_{80-x}-Te_{20}-Sb_x (x = 0, 2, 4, 6, 8 and 10 at.%) of bulk chalcogenide samples were prepared according to the conventional melt-quenched technique. The constituents' elements these compositions of high-purity (5N, Aldrich and Sigma chemical company) were weighed according to their atomic percentage and placed together in a precleaned and outgassed silica ampoule, which was evacuated to a pressure of about $10^{-4}Pa$ and then sealed. The synthesis was performed in a programmable rocking furnace and slowly heated up to approximately $1223C$ with the temperature ramp about $5C/min$, for about $24h$.

During the melt process, the ampoule was inverted at regular time intervals ($1h$) so that the amorphous solid will be homogenous and isotropic. After the synthesis,the melt was quenched rapidly in ice water at $273K$ to obtain the $Se-Te-Sb$ glassy alloy. Then the solid was broken along its natural stress line into smaller pieces suitable for grinding.

The elemental composition of the samples was analyzed by using energy dispersive X-ray spectrometer unit $(EDXS)$ interfaced with a scanning electron microscope, $SEM(JOELXL)$ operating an accelerating voltage of $30kV$. The relative error of determining the indicated elements does not exceed 4% . X-ray powder diffraction (XRD) Philips diffractometry (1710), with $Cu-K_{\alpha 1}$ radiation ($\lambda = 1.54056A^o$) have been used to examine the amorphous nature of the Se_{80}-x-Te_{20}-Sb_x (x = 0, 2, 4, 6, 8 and 10 at.%) compositions.

The data collection was performed by step scan mode, in a 2θ range between 5^o and 80^o with step-size of 0.02 and step time of 0.6 seconds. Pure Silicon Si 99.9999% was used as an internal standard. The calorimetric measurements were carried out in a differential scanning calorimeter Shimadzu 50 with an accuracy of $.1K$. The calorimeter was calibrated, for each heating rate, using well-known melting temperatures and melting enthalpies of zinc and indium supplied with the instrument. Twenty mg powdered samples, crimped into aluminum pans, were scanned at different heating rates (β = 5, 10, 20, 30 and 40 K/min). The temperatures of the glass transition, T_g, the crystallization extrapolated onset, T_{in}, the crystallization peak, T_p and the melting temperature T_m were determined with an accuracy of K.

3 Theoretical Basics

According to the formal theory of transformation kinetics as developed by Johnson and *Mehl* [24] and *Avrami* [25], the evolution with time, t, of the volume fraction crystallized,α, in terms of the crystal growth rate,w defined as

$$\alpha = 1 - exp[-g(\int_0^t w(t^{'})dt^{'})^n] \quad (1)$$

Here,g is a geometric factor and n, an exponent, which depends on the mechanism of transformation. In Eq. (1) it is assumed that the nucleation process takes place early in the transformation and the nucleation rate is zero thereafter. This process of heterogeneous nucleation has been considered as site saturation [26]. Over a sufficiently limited range of temperature ,w may be described in a zeroth-order approximation by

$w = w_o exp(\frac{-E_c}{RT})$

where E_c is the effective activation energy,w_0, a pre-exponential factor, and R is the ideal gas constant. And by assuming the heating rate$\beta = dT/dt.Eq.(1)$ becomes

$$\alpha = 1 - exp[(-g(w)/\beta)^n(\int_0^t exp(y^{'})d(T^{'}))^n]$$
$$= 1 - exp(-PI^n) \quad (2)$$

where $y^{'} = E_c/RT^{'}$ and the magnitude values which correspond to the maximum crystallization rate are denoted by subscript $'p'$. The integral I can be represented, according to the literature [27], by the sum of the alternating series:

$S(y^{'}) = \frac{-e^{-y^{'}}}{y^{'2}} \sum_{k=0}^{\infty} \frac{(-1)^k(k+1)!}{y^{'k}}$

it is possible to use only the first two terms of this series without making any appreciable error, the integral I becomes as ,$I = (RT^2/E)exp(-E/RT)$ if it is assumed that $T_0 << T$(T_0 is the starting temperature), so that y_0 can be taken as infinity, Substituting the last expression of I in Eq. (2), one obtain the volume fraction crystallized as:

$$\alpha = 1 - exp(-J(\frac{KT^2}{\beta}))^n \quad (3)$$

where J is a parameter given by $J = w(R/E)^n$ and K is the reaction rate constant The crystallization rate is obtained by differentiating Eq. (3) with respect to time

$$\frac{d\alpha}{dt} = \frac{Jn}{\beta}(1-\alpha)(\frac{KT^2}{\beta})^{n-1}(2\beta TK + T^2\frac{dk}{dt}) \quad (4)$$

The maximum crystallization rate is found by making $d^2\alpha/dt^2 = 0$,thus obtaining the relationship:

$$y_b = -ln(1-\alpha_p) = J(\frac{K_p T_p^2}{\beta})$$
$$= 1 - \frac{2}{n}(1+\frac{E}{RT_p})(2+\frac{E}{RT_p})^{-2} \quad (5)$$

Bearing in mind that in most crystallization reactions $E/RT_p >> 1$ (usually $E/RT_p \geq 25$), Eq. (5) can be rewritten in a logarithmic form as

$$ln(\frac{T_p^2}{\beta}) = \frac{E_c}{RT_p - lnh,}h = J = ^{1/2} K_0 \quad (6)$$

A linear relationship, which makes it is possible to calculate the kinetic parameter E_c and h.It is possible now to obtain the kinetic exponent n, introducing the expression $J^{1/n}K_pT_p^2$ to Eq. (4). One can obtain the relation:

$$n = (dx/dt)_p RT_p^2(0.37\beta E)^{-1} \quad (7)$$

4 Results and discussion

In order to investigate crystallization kinetics of Se_{80-x}-Te_{20}-Sb_x (x = 0, 2, 4, 6, 8 and 10 at.%) chalcogenide glasses, *DSC* experiments were carried out at different heating rates from 5-40 K/min. Figure (1) shows the *DSC* traces of the as prepared Se_{80-x}-Te_{20}-Sb_x compositions at heating rate β= 10 K/min. It is easily seen, at first an endothermic peak, which at its beginning the glass transition temperature T_g can be determined, secondly it is clearly regarding an exothermic peak, its beginning represents the initial temperature of crystallization T_i, its top represents the crystallization temperature T_p, and its end represents the T_f temperature at which crystallization completed. Numerical values of these characteristic temperatures are given in *table*.1. The variation of T_g with various compositions of Se_{80-x}-Te_{20}-Sb_x is shown obviously in *table*.1. It is obviously shown that Tg increases with the addition of *Sb* which may be explained by considering the structural change due to the introduction of *Sb* atoms. Glassy Se shows both chain and ring structures [28]. An introduction of *Te* decreases the Se ring concentration favoring *Se-Te* mixed rings. A slight increase in polymeric chain of *Se* is also observed. When *Sb* added to the above system may break the *Se-Te* chains or *Se-Te* mixed rings to satisfy its coordination number and form a cross linked structure. The addition of *Sb* also causes a decrease of Se_8 rings and increase chain length [28,29,30]. Hence Tg increases with increasing *Sb* concentration.

4.1 Compositional dependence of activation energies for glass transition E_g and for crystallization E_c

The activation energy of glass transition was determined using the values of T_g according to their corresponding heating rates across Kissinger relation, which basically derived for the crystallization process and suggested to be valid for the glass transition [27]. This relation given by:

$$ln(\frac{T_g^2}{\beta}) = \frac{E_g}{RT_g} + const \quad (8)$$

Where R is the universal gas constant. Fig. (2). shows the relation between $ln(T_g^2/\beta)$ versus $(1/T_g)$, the values of of Eg obtained from the slope of the straight line corresponding to each specimen. These values shown in table (1) give increasing trend of Eg with increases *Sb* contents. Fig. (3) shows the E_g increases with increasing *Sb* contents. This trend can be explained in terms the average coordination number. The coordination numbers of the involved elements Se, Te and Sb are 2, 2, 3 respectively, since when *Se* is replaced by *Sb* the average coordination number will increase, which leads an increasing in E_g. The average coordination number Z, of Se_x-Te_y-Sb_z ternary compound $(x + y + z = 1)$ can be expressed as [31]:

$$Z = (xCN(Se)) + yCN(Te) + zCN(Sb) \quad (9)$$

The calculated values of Z of Se_{80-x}-Te_{20}-Sb_x(x = 0, 2, 4, 6, 8 and 10 at. %) samples are listed in table (1).

It has been pointed out [32] that in a crystallization process, two types of activation energies have to be considered: activation energy for nucleation En and activation energy for growth EG. The activation energy for the whole crystallization process is called the activation energy of crystallization E_c. For the evaluation of the activation energy of crystallization E_c , using the variation of T_p with βaccording to the relation mentioned by Eq. (6). A plot of $(ln\frac{T_p^2}{\beta})$versus $1/T_p$ has been drawn for different compositions showing the straight regression line in Fig. (4). The activation energy, E_c given by the slope of the straight line. Fig. (5) shows the values of E_c as a function of *Sb* content. It is observed that, E_c increase with increasing antimony content within the composition, it can be explained as that the values of atomic weight of *Sb* (121.7 gm mol^{-1}) are more than that of Se (78.9 gm mol^{-1}). In the present work *Sb* is added to the binary *Se-Te* alloy at the cost of selenium. Thus the mean atomic weight of ternary alloys due to which an increase in the nucleation and growth rate is possible, and hence an increasing of crystallization energy was observed as *Sb* content was increased.

4.2 Crystallization rate and Avrami index

According to aforementioned theory of transformation kinetics as developed by *Johnson* and *Mehl* [24] and Avrami [25], an interpretation of *DTA* results was provided. The crystallized fraction x at a temperature T is given by $x = A_T/A$, where A is the total area of the exothermic peak between T_i (the initial temperature of crystallization) and T_f (the temperature at which crystallization is completed), A_T is the area between Ti and T, as shown in fig. (6) for the $Se_{76}Te_{20}Sb_4$ composition The graphical representation of the volume crystallized fraction of $Se_{80-x}Te_{20}Sb_x$ glasses at different heating rates shows a typical sigmoid curve as a function of temperature in crystallization reactions [33,34,35] as shown in Fig. 7(a, b) for the $Se_{80-x}Te_{20}Sb_x$ glassy compositions for x = 0 and 10 at. % respectively. The

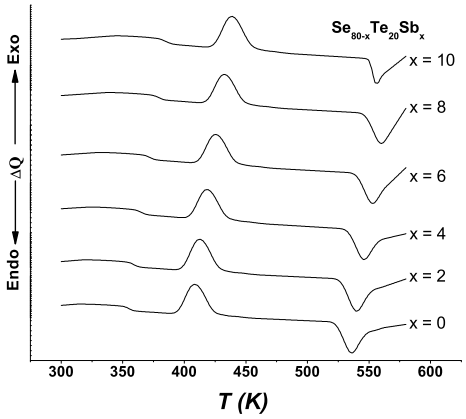

Fig. 1: The *DSC* traces of the as prepared $Se_{80-x}Te_{20}Sb_x$ (x = 0, 2, 4, 6, 8, 10) compositions at heating rate β = 10 *K/min*. (demonstrating the characteristic temperatures as referred by arrows)

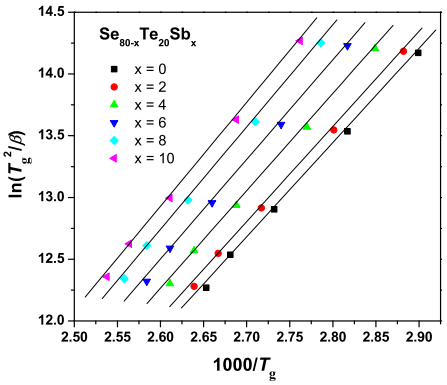

Fig. 2: Plots of $Ln(\frac{T_g^2}{\beta})$ versus $(1/T_g)$ of $Se_{80-x}Te_{20}Sb_x$ (x = 0, 2, 4, 6, 8, 10) glassy alloys and straight regression lines for all these alloys.

ratio between the ordinates of the *DTA* and the total area of the peak gives the corresponding crystallization rates, that is make possible to build the curves of the exothermal peaks represented in Fig. 8(a, b) for *Sb* content with $x = x = 0$ and10 at. % respectively.It is obviously observed that the $(dx/dt)p$ increase as well as heating rate, the same manner repeated for all the compositions which is a property that has been widely discussed by the

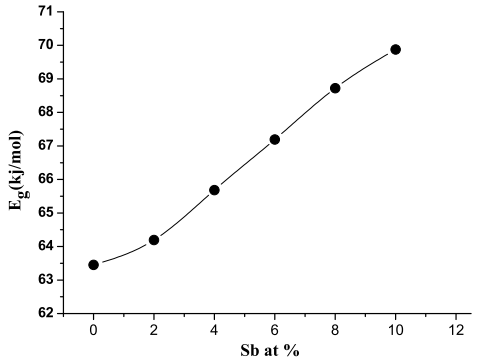

Fig. 3: The values of the activation energies $E_g$of glass transition as a function of *Sb* content.

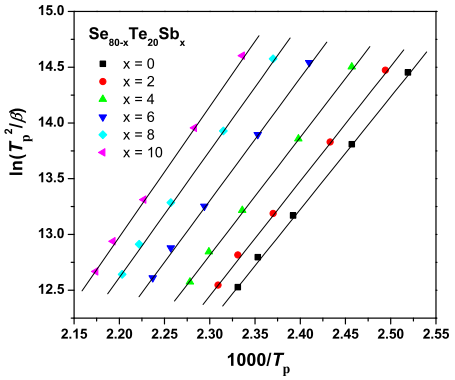

Fig. 4: Plots of $Ln(\frac{T_g^2}{\beta})$ versus $(1/T_p)$ of $Se_{80-x}Te_{20}Sb_x$ (x = 0, 2, 4, 6, 8, 10) glassy alloys and straight regression lines for all these alloys.

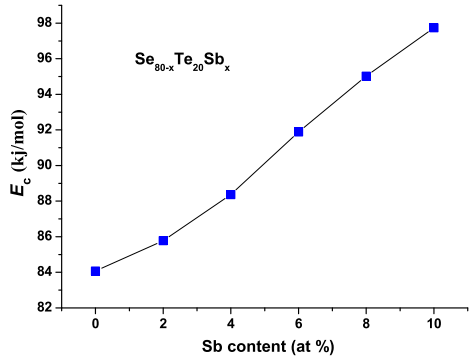

Fig. 5: The values of the activation energies of crystallization E_c as a function of *Sb* content.

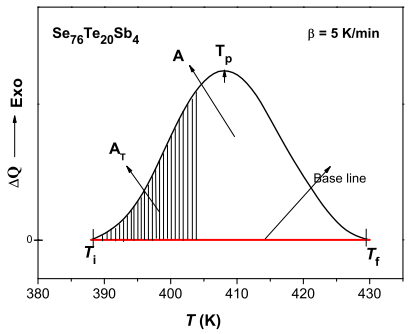

Fig. 6: *DSC* diagram for $Se_{76}Te_{20}Sb_4$ at at heating rate β = 5 *K/min*, the hatched area A_T shows between T_i and T_f of the peak

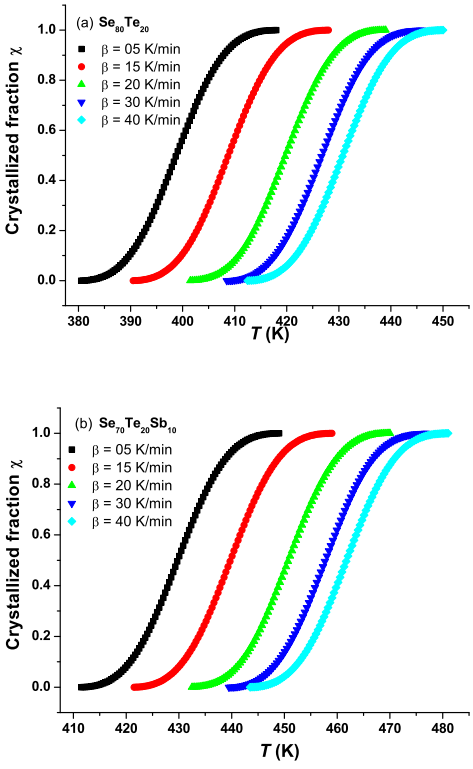

Fig. 7: (a,b) :crystallized fraction x as a function of temperature for $Se_{80-x}Te_{20}Sb_x$ (x = 0 and 10) glassy alloys respectively.

literature [36]. From the experimental values of $(dx/dt)p$ (listed in table.2) and values of activation energies E_c (shown by table 1), one can calculate the kinetic exponent n by using equation (7) The$n$ values for the glasses that are calculated are listed in table (1). Taking into account the experimental error, the values of are close to 2 for $Se_{20}Te_{80}$ (with x = 0) and close to 3 for all the remaining compositions (with x = 2, 4, 6, 8, 10). The kinetic exponent was deduced on the basis of the mechanism of crystallization [**?**]. According to Mahadevan et al [32], n may be $4,3,2,or1$, which are related to the different glass-crystal transformation mechanisms: $n = 4$, volume nucleation, three-dimensional growth; $n = 3$, volume nucleation, two dimensional growth; $n = 2$, volume nucleation, one dimensional growth; $n = 1$, surface nucleation, one dimensional growth from surface to the inside. Therefore, bearing in mind the above obtained mean value, = 2 means volume nucleation, one dimensional growth for the $Se_{80}Te_{20}$ and = 3 for the crystallization peaks means volume nucleation, two dimensional growth for all the remaining compositions. Regarding the values of n [37] it is observed that at non integer values of n for $x = 0,2,4$ means the two and three dimensional growth working in the same time during the amorphous crystalline transformation, while integer values of n means that only one mechanism (three dimensional growth) is responsible for the crystallization process of the $(x = 6,8,10)$. It was supposed [38] that small antimony addition (2 at.%) leads to cross-linking of the chains to some extent, creating a two-dimensional network. Further addition of antimony breaks the chains and forms large number of smaller chains. The natural tendency of antimony atoms is to create either a trigonal, bipyramidal or octagonal environmental with more or less covalent bonds. The *Sb* contributes to change the weak bonding between the $Se-Te$ polymeric chains to relatively strong covalent bonds [38]. Three-dimensional growth responsible for crystallization of the $Se_{80-x}Te_{20}Sb_x$ (x = 6, 8 and 10) may attributed to the formation of ternary crystalline phase such as Sb_2TeSe_2.

4.3 Identification of crystalline phases by thermal treatment using X-ray diffraction

The X-ray diffraction patterns of $Se_{80}Te_{20}$, $Se_{78}Te_{20}Sb_2$, $Se_{74}Te_{20}Sb_6$ and $Se_{70}Te_{20}Sb_{10}$ alloys annealed at temperatures beyond the peak of crystallization temperatures with a heating rate of $10Kmin^{-1}$ for $2h$ are shown in Fig. (9). The diffractograms of the transformed material after the crystallization process suggest the presence of microcrystallites of two phase of binary $Se_{80}Te_{20}$ according to *JCPDS* of $Se_{7.68}Te_{0.32}$ (01-087-2413) and $Se_{5.95}Te_{1.05}$ (01-087-2414) and three phases for ternary *Se-Te-Sb*. From the *JCPDS* files these peaks can be identified as,(1) Antimony Tellurium Selenide, Sb_2TeSe_2 $(40-1211)$, (2) Antimony, *Sb* (card No. $5-0562$), and (3) Selenium, *Se* (card No. $1-0848$), while there remains also additional amorphous phases represented by the remaining two broad humps as shown in Fig. (9). Regarding ternary crystalline phase Sb_2TeSe_2 for all the compositions except $Se_{80}Te_{20}$, confirms the last determined values of $\langle n \rangle$ which predict one dimensional

Table 1: The values of thermal parameters of glass transition temperature T_g, onset temperature of crystallization T_{in}, crystallization temperature T_p of $Se_{80-x}Te_{20}Sb_x$ $(0 \leq x \leq 10)$ alloys with different heating rates . The kinetic parameters E_g and E_c according to the text, and the corresponding average coordination number Z.

	β	T_g (K)	T_{in}(K)	T_p(K)	E_g (kj/mol)	E_c (kj/mol)	Z
x=0							
	5	345	380	397	63.452	84.075	2
	10	355	390	407			
	20	366	401	418			
	30	373	408	425			
	40	377	412	429			
x=2							
	5	347	385	401	64.192	85.78	2.02
	10	357	395	411			
	20	368	406	422			
	30	375	413	429			
	40	379	417	433			
x=4							
	5	351	391	407	65.684	88.371	2.04
	10	361	401	417			
	20	372	412	428			
	30	379	419	435			
	40	383	423	439			
x=6							
	5	355	398	415	67.194	91.886	2.06
	10	365	408	425			
	20	376	419	436			
	30	383	426	443			
	40	387	430	447			
x=8							
	5	359	405	422	68.72	95.017	2.08
	10	369	415	432			
	20	380	426	443			
	30	387	433	450			
	40	391	437	454			
x=10							
	5	362	411	428	69.876	97.742	2.1
	10	372	421	438			
	20	383	432	449			
	30	390	439	456			
	40	394	443	460			

growth for $Se_{80}Te_{20}$ and two dimensional growths for all the remaining compositions. Intensity differences between the dominant peaks of each phase can be observed; hence the same crystalline phases could be identified in all the samples.

5 Conclusions

Crystallization kinetics study of the Se_{80-x}-Te_{20}-Sb_x (x = 0, 2, 4, 6, 8, and 10) glassy compositions have resulted in the following: 1− The glass transition temperature, activation energy of glass transition and activation energy of crystallization were increased with increasing the antimony percent within the composition. 2− According to the mean values of Avrami indices, $< n >$, $Se_{20}Te_{80}$ has volume nucleation, one dimensional growth and the other remaining compositions have volume nucleation, two dimensional growth. 3− The diffractograms of the transformed material after the crystallization process suggest the presence of microcrystallites of two phases of $Se_{7.68}Te_{0.32}$ and $Se_{5.95}Te_{1.05}$ for binary $Se_{80}Te_{20}$ and three phases for ternary *Se-Te-Sb*. The X-rays diffraction demonstrate the existence of Sb_2TeSe_2ternary crystalline phase in all the compositions except $Se_{20}Te_{80}$, which confirm the results implied by the values of $< n >$

Table 2: Maximum crystallization rate ($\frac{dx}{dt} \times 10^{-3} S^{-1}$) , kinetic exponent n and average kinetic exponent $\langle n \rangle$ for $Se_{80-x}Te_{20}Sb_x$ ($0 \leq x \leq 10$) alloys with different heating rates β .

x	0		2		4		6		8		10	
$\beta(K/min)$	$\frac{dx}{dt}$	n	$\frac{dx}{dt}$	n	$\frac{dx}{dt}$	n	$\frac{dx}{dt}$	n	$\frac{dx}{dt}$	n	$\frac{dx}{dt}$	n
5	4.374	2.212	5.269	2.664	5.721	2.893	5.981	3.024	6.157	3.113	6.236	3.153
10	8.319	2.211	10.03	2.664	10.9	2.892	11.4	3.023	11.75	3.112	11.91	3.152
20	15.8	2.214	19.04	2.666	20.71	2.895	21.69	3.026	22.36	3.115	22.68	3.155
30	22.91	2.213	27.63	2.665	30.06	2.894	31.5	3.025	32.5	3.114	32.97	3.154
40	29.95	2.211	36.14	2.664	39.32	2.892	41.23	3.023	42.54	3.112	43.18	3.152
$\langle n \rangle$		2.212		2.665		2.893		3.024		3.113		3.153

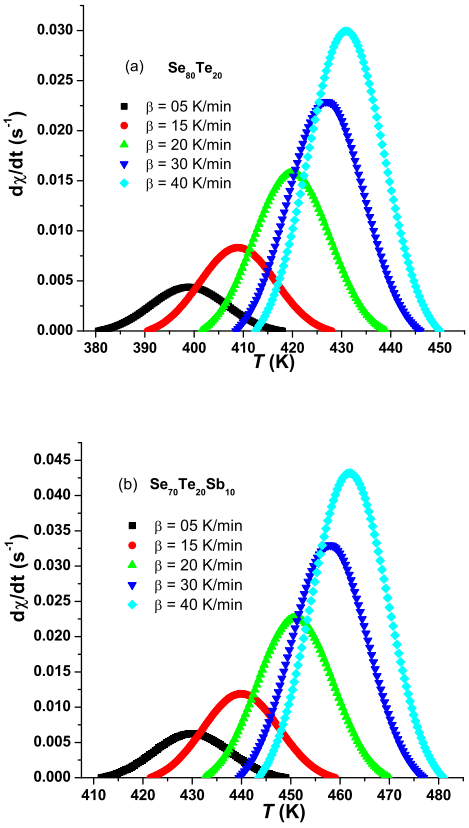

Fig. 8: (a,b) : Crystallization rate versus temperature of the exothermal peaks at different heating rates of $Se_{80-x}Te_{20}Sb_x$ (x = 0 and 10) glassy alloys respectively.

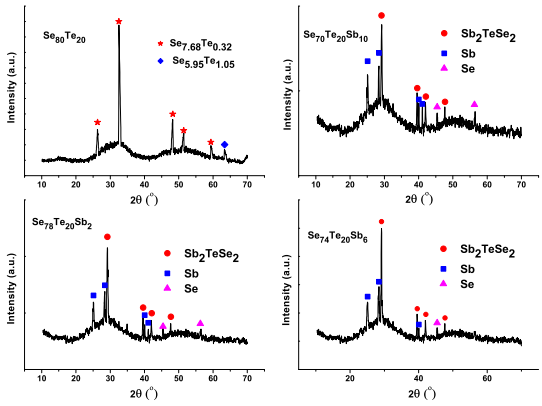

Fig. 9: The X-ray diffraction patterns of crystallized $Se_{80-x}Te_{20}Sb_x$ (x = 0, 2, 6, 10) alloys.

References

[1] L. Heireche, M. Heireche, M. Belhadji, *Journal of Crystallization Process and Technology*, **4**, 111-120 (2014)

[2] L. Heireche and M. Belhadji, *Journal of Optoelectronics and Advanced Materials*, **11**, 1058-1066 (2009).

[3] E. R. Shaaban, M. T. Dessouky, A. M. Abousehly, *Philosophical Magazine*, **7**, 1099-1112 (2008).

[4] S. F. Naqvi, N.S. Saxena, K. Sharma and D. Bhandari, *Journal of Alloys and Compounds*, **506**, 956-962 (2010).

[5] F. A. Abdel-Wahab, S. A. El-Hakim and M. F. Kotkata, *Physica B:Condensed Matter*, **506**, 38-43 (2005).

[6] E. R. Shaaban, I. Kansal, M. Shapaan and J. M. F. Ferreira, *Journal of Thermal Analysis and Calorimetry*, **98**, 347-354 (2009).

[7] M. A. Majeed Khan, S Kumar, M Husain and M Zulfequar, *Materials Letters*, **6**, 1572-1574 (2008).

[8] A. H. Ammar, N. M. Abdel-Moniem, A. A. M. Farag and E.-S. M. Farag, *Physica B*, **407**, 356-360 (2012).

[9] E. R. Shaaban, I. B. I. Tomsah, *Journal of Thermal Analysis and Calorimetry*, **105**, 191-198 (2011).

[10] J. Zhang, S. Y. Zhang, J. J. Xu and H. Y. Chen, *Chinese Chemical Letters*, **15**, 1345 (2004).

[11] N. Yamada, E. Ohno, N. Akahira, K. Nishiuchi, K. Nagata and M. Takao, *Japanese Journal of Applied Physics*, **26**, 61-66 (1987).

[12] E. R. Shaaban, M. T. Dessouky and A. M. Abousehly, *Journal of Physics:condensed Matter*, **19**, 96212-96212 (2007).

[13] L. Le Neindre, F. Smektala, K. Le Foulgoc and X. H. Zhang, *Journal of Non-Crystalline Solids*, **242**, 99-103 (1998).

[14] T. Akiyama, M. Uno, H. Kitaura, K. Narumi, R. Kojima, K. Nishiuchi and N. Yamada , *Japanese Journal of Applied Physics*, **40**, 1598-1603 (2001).
[15] T. Ohta, *Journal of Optoelectronics and Advanced Materials*, **3**, 609-626 (2001).
[16] N. Suri, K. S. Bindra, P. Kumar, R. Thangaraj, Journal of Non-Crystalline Solids, **353**, 1264-1267 (2007).
[17] S . O Kasap, C. Juhasz, *Journal of Materials Science*, **21**, 1329-1340 (1986).
[18] S . K. Tripathi and A. Kumar, *Journal of Electronic Materials*, **17**, 45-51 (1988).
[19] R. Arora and A. Kumar, *Physica Status Solidi (A)*, **115**, 307-314 (1989).
[20] A. H. Abouelela, M. K. EL-Mously and K. S. Abdu, *Journal of Materials Science*, **15**, 871-874 (1980).
[21] C. T. Moynihan, A. J. Easteal, J. Wilder and J. Tucker, *The Journal of Physical Chemistry*, **78**, 2673-2677 (1974).
[22] P. Agarwal, S. Goel, J. S. P. Rai and A. Kumar, *Physica Status Solidi (A)*, **127**, 363-369 (1991).
[23] A. Kumar, PhD Thesis, Punjab University, 1979.
[24] A. Marotta, S. Saiello, F. Branda, A. Buri, *Journal of Materials Science*, **17**, 105-108 (1982).
[25] M. Avrami, *The Journal of Chemical Physics*, **7**, 1103-1112 (1939).
[26] S. A. Khan, M. Zulfequar, M. Husain, *Solid State Communications*, **123**, 463-468 (2002).
[27] H. E. Kissinger, *Analytical Chemistry*, **29**, 1702-1706 (1957).
[28] J . Schottmiller, M. Tabak, G. Lucovsky and A. Ward, *Journal of Non-Crystalline Solids*, **4**, 80-96 (1970).
[29] A. Eisenberg, *POLYMER LETTERS*, **1**, 177-179 (1963).
[30] K. Nakayama, K. Kojima, I. Tamaru, Y. Masaki, A. Kitagawa, M. Suzuki, *Journal of Non-Crystalline Solids*, **758**, 198-200 (1996).
[31] A. H. Ammar, A. M. Farid, S. S. Fouad, *Physica B: Condensed Matter*,**307**, 64-71 (2001).
[32] S. Mahadevan, A. Giridhar and A. K. Singh, *Journal of Non-Crystalline Solids*, **88**, 11-34 (1986).
[33] C. Wagner, P. Villanes, J Vazquez, R. Jirnenex-Caray, *Materials Letters*, **15**, 370-375 (1993).
[34] A. Goel, E. R. Shaaban, M. J. Ribeiro, F. C. L. Melo, J. M. F. Ferreira, *Journal Of Physics: Condensed Matter*, **19**, 386231-386245 (2007).
[35] W. A. Johnson, R. F. Mehl, *Trans Am Inst Min Met Eng.* , **135**, 416-58 (1939).
[36] K. Matusita, S. Saka, *Journal of Non-Crystalline Solids*, **38&39**, 741-746 (1980).
[37] R. M. Mehra, A. Gurinder, A. Ganjoo, R. Singh, P. C. Mathur, *Physica Status Solidi (A)*, **124**, 51-53 (1991).
[38] M. Mehdi, G. Brun, J. C. Tedenac, *Journal Of Materials Science*, **30**, 5259-5262 (1995).